MR-driven Computational Fluid Dynamics

J-F. Nielsen[1], and K. S. Nayak[2]

[1]Biomedical Engineering, University of Michigan, Ann Arbor, MI, United States, [2]Electrical Engineering, University of Southern California, Los Angeles, CA

Introduction: Knowledge of blood flow patterns in the human body is a critical component in cardiovascular disease diagnosis. In-vivo blood flow is typically assessed either by 3D phase-contrast MRI [1], or by Computational Fluid Dynamics (CFD) calculations [2]. MRI measurements are direct, but offer limited spatio-temporal resolution. Conventional CFD calculations offer "infinite" spatial resolution, but rely on the accuracy of the assumed fluid properties and boundary conditions (e.g. blood viscosity, inlet/outlet flow, and the location and compliance of the vessel wall). We propose a hybrid MRI/CFD approach that integrates low-resolution MRI flow measurements directly into the CFD solver. The feasibility of the proposed "MR-driven CFD" approach is demonstrated in the carotid bifurcation of one healthy volunteer. We show that MR-driven CFD has a regularizing effect on the flow fields obtained with MRI alone, and produces flow patterns that are in better agreement with direct MRI measurements than CFD alone.

Methods: Experiments were performed on a GE Signa 3T EXCITE HD system (4 G/cm and 15 G/cm/ms max gradient amplitude and slew rate), using a 4-channel receive coil array. Four time-resolved 3DFT FGRE image volumes were acquired in the carotid artery in a healthy volunteer (1x1x2.5 mm^3 voxel size; FOV 16x12x6 cm^3; TR=7.0 ms; flip angle=15°; temporal resolution 56 ms; scan time = 7 min per scan). A bipolar velocity-encoding gradient pulse (VENC=1.6 m/s) was placed on the x, y, or z-gradient axis, or was turned off.

MR-driven CFD calculations were performed using a modified version of the SIMPLER algorithm [3], an iterative routine for solving the discretized (non-linear, and coupled) momentum and continuity equations. Newtonian, incompressible flow was assumed. At each iteration i, the equations are linearized using the flow field estimate at the previous iteration, which produces a square system matrix $\mathbf{A}_{u,i}$ for each velocity component $u = v_x$, v_y, or v_z. Our approach is to add additional rows to $\mathbf{A}_{u,i}$ that incorporate MRI measurements of the velocity component u, and to solve the resulting rectangular system using the Conjugate Gradient method on the normal equations. This is possible because the velocity measured with MRI is to a good approximation equal to the average velocity within the voxel, and can hence be expressed as a simple linear combination of the velocities on the underlying CFD calculation grid. In the results presented here, only the measured v_z component (vertical in Fig. 1) was incorporated into the MR-driven CFD solver. Hence, v_x and v_y were determined solely from the momentum and continuity equations. The normal velocity (v_z) at the inlet and outlet of the calculation domain were set equal to the v_z values obtained with MRI at mid-systole. Simulations assumed a blood viscosity $\mu = 0.0027$ Pa-sec and blood density $\rho = 1060$ kg/m^3 (Reynolds number of order 1000), as well as 'no-slip' boundary conditions. A steady-state solution was obtained by carrying the simulations forward until convergence. Calculations were performed on a Cartesian grid of 1 mm isotropic resolution. All algorithms were implemented in Matlab (code is available on the authors' website).

Results: Fig. 1 compares flow fields obtained with MRI only, CFD only, and the proposed MR-driven CFD algorithm. In the carotid bifurcation, we observe that CFD tends to underestimate the flow rate, which is in qualitative agreement with a recent report on aortic blood flow [4]. MR-driven CFD brings the calculated flow fields in closer agreement with the values measured with MRI, while generally appearing less noisy than the direct MRI measurements. In the CCA, all methods produce comparable flow fields.

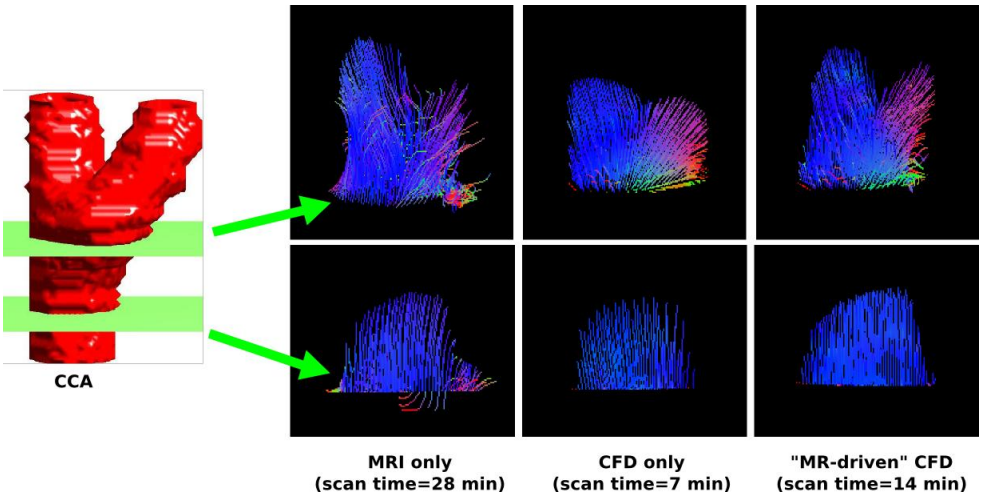

Figure 1: Pathline visualization of blood flow in the carotid bifurcation (top) and the common carotid artery (bottom), using flow fields at mid-systole obtained with 4-point phase-contrast MRI (left), CFD only (middle), and the proposed MR-driven CFD approach (right). Each line shows the path of a massless particle during the course of 60 ms (top) or 20 ms (bottom), under the assumption of a constant velocity field. Pathlines are RGB color-coded according to the local velocity direction (vertical=blue; in-plane=red and green). These flow fields were obtained from 4 (left), 1 (middle), or 2 MRI scans, corresponding to total scan times of 28, 7, and 14 min, respectively.

Discussion: In our calculated flow data, we have observed that pathlines that start out near the vessel wall sometimes leave the lumen erroneously. We believe this is related to the coarse computational grid used in this feasibility study (only 7-8 grid points span the CCA). Higher spatial resolution and/or a body-fitted non-Cartesian mesh may alleviate this issue.

In-flow signal enhancement and vessel wall/lumen signal differences were not accounted for in this work, but should in general be considered. In thick-slab 3D acquisitions, in-flow enhancement may be relatively unimportant. In acquisitions with high wall/lumen contrast (e.g. balanced SSFP), the rows representing MRI measurements of voxels that straddle the wall/lumen interface may simply be left out of the (rectangular) system matrix. In general, the proposed framework allows any combination of local MRI velocity measurements to influence the CFD solution, whether it be individual pixels, one or more 2D slices, or 3D regions-of-interest.

Conclusions: The proposed method provides a general and flexible framework for "guiding" the CFD solutions toward flow fields that are more consistent with the velocity component(s) measured with MRI than those produced by CFD alone. The underlying hypothesis to be addressed in the long-term is that MR-driven CFD provides more accurate and robust velocity field estimates compared to either MRI or CFD alone, resulting in improved estimates of clinically significant blood flow patterns and derived hemodynamic parameters such as wall shear stress.

Acknowledgments: This work was supported by the American Heart Association (POST-0625253Y) and the LA Basin Clinical Translational Science Institute.

References: [1] Markl et al, JMRI 25:824 (2007); [2] Rayz et al, J Biomech Eng 130:051011 (2008); [3] Suhas V. Patankar, "Numerical Heat Transfer and Fluid Flow" (1980); [4] Canstein et al, MRM 59:535 (2008).